Impaired GABAergic transmission disrupts normal homeostatic plasticity in cortical networks

LE ROUX Nicolas, AMAR Muriel, MOREAU Alexandre, BAUX Gérard and FOSSIER Philippe.

CNRS, Institut de Neurobiologie Alfred Fessard – FRC2118,

Laboratoire de Neurobiologie Cellulaire et Moléculaire – UPR9040,

Gif sur Yvette, F-91198, France

Abbreviated title: Cortical homeostatic plasticity requires $GABA_A$ receptor

Corresponding author : LE ROUX Nicolas, NBCM-CNRS, Gif sur Yvette, F-91198, France.

leroux@nbcm.cnrs-gif.fr

Abstract: 189 words

Text pages: 37

Figures: 7

Abstract

In the cortex, homeostatic plasticity appears as a key process for maintaining neuronal networks activity in a functional range. This phenomenon depends on close interactions between excitatory and inhibitory circuits. We previously showed that application of a high-frequency of stimulation (HFS) protocol in layer 2/3 induces parallel potentiation of excitatory and inhibitory inputs on layer 5 pyramidal neurons, leading to an unchanged excitation/inhibition (E/I) balance. These coordinated Long Term Potentiations (LTP) of excitation and inhibition correspond to homeostatic plasticity of the neuronal networks.

We showed here on the rat visual cortex, that the blockade (with gabazine, GBZ) or the over-activation (with 4,5,6,7-tetrahydroisoxazolo[5,4-c]pyridin-3-ol, THIP) of $GABA_A$ receptors enhanced the E/I balance and prevented the potentiation of excitatory and inhibitory inputs after an HFS protocol. These impairements of the GABAergic transmission led to a LTD-like (Long Term Depression) effect after an HFS protocol. We also observed that the blockade of inhibition reduced excitation (by 60 %) and conversely the blockade of excitation decreased inhibition (by 90 %). These results support the idea that inhibitory interneurons are critical for recurrent interactions underlying homeostatic plasticity in cortical networks.

Keywords: $GABA_A$ receptors, homeostatic plasticity, LTP, cortical networks.

Introduction

Layer 5 pyramidal neurons in the cortex elaborate cortical output signals as a function of the balance between excitatory and inhibitory inputs received (Marder & Prinz, 2002). This E/I balance is closely regulated in order to keep neuronal responsiveness in a functional range. An imbalance was reported to underlie various pathologies such as epilepsy or schizophrenia (Cline, 2005). The E/I balance of cortical layer 5 pyramidal neurons is dynamically maintained to a set-point composed of 20 % excitation and 80 % inhibition (Le Roux *et al.,* 2006); whereas inhibitory interneurons represents 20 % of the neuronal population of the cortex (Peters & Kara, 1985). These results highlight the particular role of inhibitory interneurons in the control of the E/I balance of layer 5 pyramidal neurons.

The dynamic equilibrium between strengths of excitatory and inhibitory inputs depends on compensatory changes between excitation and inhibition received by a cell (Turrigiano, 1999; Liu *et al.,* 2007). A deregulation of normal activity (by pharmacological treatment or visual deprivation) induces a normalization or a scaling of this activity (after 24-48h) by changes of the excitatory synaptic drive (Turrigiano *et al.,* 1998; Maffei *et al.,* 2004; 2006). This phenomenon was described in terms of homeostatic plasticity (Turrigiano & Nelson, 2004; Davis, 2006) which ensures that neurons have the ability to integrate new information, by modification of the strength of their inputs, while a stable E/I ratio is maintained.

Using a method that allows the decomposition of the response of a layer 5 pyramidal neuron, following electrical stimulation in layer 2/3, into its excitatory and inhibitory components (Borg-Graham *et al.,* 1998; Monier *et al.,* 2003) we previously showed that application of a High Frequency of Stimulation (HFS) protocol induces parallel increases of excitatory and inhibitory inputs received by layer 5 pyramidal neurons (Le Roux *et al.,* 2006). Therefore, the E/I balance was not modified, and this process corresponds to a homeostatic plasticity process

which differs from synaptic scaling because it consists of parallel and immediate changes in synaptic drives and requires synaptic NMDA receptor activation (Le Roux *et al.*, 2007).

Most of the data about homeostatic plasticity comes from work on excitatory synapses. However, in the normal functioning brain, the regulation of inhibitory synaptic strength is also important for the timing of the critical period (Freund & Gulyas, 1997; Zilberter, 2000), for the synchronization of neuronal activity (McBain & Fisahn, 2001; Freund, 2003; Tamas *et al.*, 2000) and for learning and memory (Bradler & Barrionuevo, 1989; Steele & Mauk, 1999). This inhibitory plasticity was also involved in pathological conditions such as drug abuse or epilepsy (Lu *et al.*, 2000; Nugent *et al.*, 2007). Despite this major involvement in the control of normal brain functions, mechanisms responsible for the induction of inhibitory synapses plasticity remain poorly understood (Caillard *et al.*, 1999a; 1999b; Gaiarsa *et al.*, 2002). Moreover, homeostatic plasticity is based on coordinated changes of the strength of excitatory and inhibitory synaptic drive. Therefore it is crucial to determine some key cellular mechanisms underlying the inhibitory control of activity in conditions where the interactions between excitation and inhibition remain functional.

Our aim was to determine the involvement of $GABA_A$ synaptic drive for the regulation of the cortical network activity and the homeostatic potentiation that occurred. We found that increasing $GABA_A$ receptor activation induces a disruption of the E/I balance. We show that any deregulation of the GABAergic system, due to an over-activation or a blockade of $GABA_A$ receptors, prevents normal plasticity processes induced by HFS (usually used to induce Long-Term Potentiation) and leads to a depression of excitatory and inhibitory inputs on the layer 5 pyramidal neuron, a LTD-like (Long-Term Depression-like) effect ordinarily induced by a specific protocol of stimulation.

Materials and Methods

Slice preparation

Parasagittal slices containing primary visual cortex were obtained from 18 to 25-day-old Wistar rats. In accordance with the guidelines of the American Neuroscience Association, a rat was decapitated, and its brain quickly removed and placed in chilled (5°C) artificial cerebrospinal extracellular solution. Slices of 250 µm thickness were made from the primary visual cortex, using a vibratome and then incubated for at least 1 hr at 36°C in a solution containing (in mM) : 126 NaCl, 26 $NaHCO_3$, 10 Glucose, 2 $CaCl_2$, 1.5 KCl, 1.5 $MgSO_4$ and 1.25 KH_2PO_4 (pH 7.5, 310/330 mOsm). This solution was bubbled continuously with a mixture of 95 % O_2 and 5 % CO_2.

Electrophysiological recordings and cell identification

Slices were placed on the X-Y translation stage of a Zeiss microscope, equiped with a video-enhanced differential interference contrast system, and perfused continuously. The optical monitoring of the patched cell was achieved with standard optics using 40X long-working distance water immersion lens. Layer 5 pyramidal neurons, identified from the shape of their soma and primary dendrites and from their current-induced excitability pattern, were studied using the patch-clamp technique in whole-cell configuration. Somatic whole-cell recordings were performed at room temperature using borosilicate glass pipettes (of 3-5 MΩ resistance in the bath) filled with a solution containing (in mM) : 140 K-gluconate, 10 HEPES, 4 ATP, 2 $MgCl_2$, 0.4 GTP, 0.5 EGTA (pH 7.3 adjusted with KOH, 270-290 mOsm).

Current-clamp and voltage-clamp recordings were performed using an Axopatch 1D (Axon Instruments, USA), filtered by a low-pass Bessel filter with a cut-off frequency set at 2 kHz, and digitally sampled at 4 kHz. The membrane potential was corrected off-line by about –10

mV to account for the junction potential. Estimation of the access resistance (Rs) is critical to quantitatively evaluate the relative change of input conductance in response to synaptic activation. After capacitance neutralisation, bridge balancing was done on-line under current-clamp conditions, which provided an initial estimate of Rs. The Rs value was checked and revised, as necessary off-line, by fitting the voltage response to a hyperpolarizing current pulse with the sum of two exponentials. Under voltage-clamp conditions, the holding potential was corrected off-line using this Rs value. Only cells with a resting membrane potential more negative than -55 mV and allowing recordings with Rs value lower than 25 MΩ were kept for further analysis. The firing behavior of neurons was determined in response to depolarizing current pulses ranging from –100 to 200 pA under current-clamp conditions.

The stimulating electrodes were positioned in layer 2/3. Electrical stimulations (1-10 μA, 0.2 ms duration) were delivered in this layer using 1 MΩ impedance bipolar tungsten electrodes (TST33A10KT, WPI). The intensity of the stimulation was adjusted in current-clamp conditions to induce a subthreshold postsynaptic response due to coactivation of excitatory and inhibitory circuits. Responses with antidromic spikes were discarded. Under voltage-clamp conditions, the frequency of stimulation was 0.05 Hz and five to eight trials were repeated for a given holding potential.

A control recording was made after 15 min of patch-clamp equilibration at 0.05 Hz, and then drugs were continuously perfused during 20 min, a “drug recording” was made in the same conditions. We next applied a HFS (high frequency of stimulation) protocol in order to induce long term modifications of synaptic strengths in the recruited circuits. The HFS protocol was elicited with theta burst stimulation (TBS) known to induce long term potentiation (LTP) at the synaptic level. It consists of 3 trains of 13 bursts applied at a frequency of 5 Hz, each burst containing 4 pulses at 100 Hz (Abraham & Huggett, 1997). Recordings were made at 0.05 Hz after 15, 30, 45 and 60 min application of HFS protocol.

Drugs

Agonist and antagonists of $GABA_A$ receptors: bicuculline, 4,5,6,7 terahydroisoxazolo[5,4-*c*]pyridine-3-ol (THIP or Gaboxadol) and gabazine (SR95531) purchased from Sigma (St-Louis, Missouri) were dissolved in the perfusate for at least 15 min before recordings.

Synaptic responses analysis

Data were analyzed off-line with specialized software (Acquis1^{TM} and Elphy^{TM}: written by Gérard Sadoc, Biologic UNIC–CNRS, France). The method is based on the continuous measurement of conductance dynamics during stimulus-evoked synaptic response, as primarily described *in vivo* on cat cortex (Borg-Graham *et al.,* 1998; Monier *et al.,* 2003) and was recently validated on rat visual cortex (Le Roux *et al.,* 2006). This method received further validation on other experimental models (Shu *et al.,* 2003; Wehr and Zador 2003; Higley and Contreras 2006; Cruikshank *et al.,* 2007). Evoked synaptic currents were measured and averaged at a given holding potential. In I-V curves for every possible delay (t), the value of holding potential (Vh) was corrected (Vhc) from the ohmic drop due to the leakage current through Rs, by the equation: Vhc(t) = Vh(t) – I(t) x Rs. An average estimate of the input conductance waveform of the cell was calculated from the best linear fit (mean least square criterion) of the I-V curve for each delay (t) following the stimulation onset. Only cells showing a Pearson correlation coefficient for the I-V linear regression higher than 0.95 between –90 and –40 mV were considered to calculate the conductance change of the recorded pyramidal neuron from the slope of the linear regression.

The evoked synaptic conductance term (gT(t)) was derived from the input conductance by subtracting the resting conductance (g_{rest}). Under our experimental conditions, the global spontaneous activity was very weak and thus, the synaptic activity at rest was null.

Consequently, the g_{rest} value was estimated 90 ms before the electrical stimulation. The apparent reversal potential of the synaptic current at the soma (Esyn(t)) was taken as the voltage abscissa of the intersection point between the I-V curve obtained at a given time (t) and that determined at rest. Assuming that the evoked somatic conductance change reflects the composite synaptic input reaching the soma, Esyn(t) characterizes the stimulation-locked dynamics of the balance between excitation and inhibition.

Decomposition of the synaptic conductance

To decompose the global evoked synaptic conductance (gT(t)) into excitatory and inhibitory components (gE(t) and gI(t)), we used the following simplifications:

$Isyn(t) = gE(t)\,(Esyn(t) - Eexc) + gI(t)\,(Esyn(t) - Einh)$ and $gT(t) = gE(t) + gI(t)$

where Isyn(t) is the total synaptic current, Esyn(t) is the apparent reversal potential at the soma (see the previous paragraph), gE(t) and gI(t) are excitatory and inhibitory conductances respectively and Eexc and Einh are the reversal potentials for excitation and inhibition. Values of these reversal potentials were equal to 0 mV for excitation (Eexc) and to -80 mV for inhibition (Einh), lumping the combined effects of the activation of $GABA_A$ and $GABA_B$ receptors in a single inhibitory component potential (Anderson *et al.,* 2000; Borg-Graham, 2001; Monier *et al.,* 2003; 2008). The value of -80 mV used in the decomposition method is the reversal potential of $GABA_A$ (and not an intermediate value between $GABA_A$ and $GABA_B$) because in the presence of QX314 (which blocks K^+ efflux), no significative variation of the synaptic response was observed. Moreover, Monier *et al.* (2008) showed that the $GABA_B$ conductance change never exceeded more than 2% of the global conductance change.

We showed that the I/V curve in the presence of excitatory synaptic transmission blockers (CNQX, D-AP5) is linear between -80 to +10 mV with a reversal potential equal to -80 mV

(Le Roux *et al.,* 2006). In the presence of bicuculline that blocks inhibitory inputs on the layer 5 pyramidal neuron, the I/V curve for excitation is linear between -80 to +10 mV with a reversal potential equal to 0 mV (data not shown) as already shown by other studies (Wehr & Zador, 2003; Higley & Contreras, 2006). Under our experimental conditions of stimulation of cortical layers leading to subthreshold postsynaptic responses, Esyn(t) which was extrapolated from I-V curves took any intermediate value between -80 mV and -40 mV (Le Roux *et al.,* 2006; supplementary data) *i.e*. within the limits of our voltage excursion (-90 to -40 mV) corresponding to the linearity of I-V curves and between the respective values of Einh and Eexc in such a way that the mathematical conditions of the oversimplification used to calculate gI(t) and gE(t) were fulfilled.

Like all somatic recordings, our recordings cannot make rigorous estimates of synaptic events in the distal dendrites and the conductance estimates are ratios of the overall excitatory and inhibitory drive contained in the local network stimulated (Haider *et al.,* 2006). However, our measurements give relative changes in conductance magnitude which reflect the cumulative contributions of excitation and inhibition arriving at proximal portions of the neuron. These relative conductance changes at the somatic level define a narrow window over which input integration and spike output can occur (Higley & Contreras, 2006).

To quantify the synaptic conductance changes, the integral (Int) over a time window of 200 ms was calculated for the total conductance change (IntgT) and for the excitatory and inhibitory conductance changes (IntgE and IntgI, respectively). The contribution of each component was expressed by the ratio of its integral value (IntgE or IntgI) to that of total conductance change (IntgT).

Reconstitution of the membrane potential

The dynamics of the membrane potential (VrecT) was reconstituted from the experimentally derived excitatory and inhibitory conductance profiles, on the basis of the prediction given by the combination of the different synaptic activation sources:

$$\frac{dVm(t)}{dt} = \frac{g_{rest} + gT(t)}{\tau\, g_{rest}} \left(\frac{g_{rest}\, E_{rest} + gT(t)Esyn\,(t)}{g_{rest} + gT(t)} - Vm(t) \right)$$

where τ is the membrane time constant measured at rest by injecting a 50 pA hyperpolarizing current step and E_{rest} is the resting potential.

Statistical analysis

Data are expressed as the mean ± the standard deviation of the mean (SD) of n cells. Statistical analyses were performed using the parametrical *t*-test for paired samples. In this latter case, data were expressed as percents of control values. Data were considered statistically significant for $p \leq 0.05$ (*), $p \leq 0.01$ (**) and $p \leq 0.001$ (***).

Results

Effects of the blockade of $GABA_A$ receptors on the E/I balance

To further characterize the involvement of $GABA_A$ receptors in the homeostatic regulation process of the E/I balance in visual cortex previously reported (Le Roux *et al.,* 2006), we first blocked $GABA_A$ receptors using gabazine (GBZ), a specific blocker of $GABA_A$ receptors. We used two concentrations of GBZ which do not fully block $GABA_A$ receptors (Cope *et al.,* 2005) in order to determine the limits in which the inhibitory control of the E/I balance remains functional.

Representative recordings of current responses of a layer 5 pyramidal neuron to layer 2/3 stimulations are presented in Figure 1A under control conditions and 20 min after application of 30 nM GBZ, a low concentration which is supposed to block extrasynaptic $GABA_A$ receptors (Cope *et al.,* 2005). The total conductance change (gT) of the pyramidal neuron (Fig. 1A medium traces), calculated from current recordings (see Methods) did not significantly change in the presence of GBZ. Decomposition of gT into its excitatory and inhibitory components (gE and gI, respectively) shows no significant variation of either component (Fig. 1A, lower traces). This observation was confirmed by the statistical analysis of the neuronal population (n = 11). Relative conductance changes are presented in Figure 1B (left part): IntgT (black bars), IntgE (dark grey bars) and IntgI (light grey bars) were not significantly modified. Under these conditions, excitatory and inhibitory conductance changes, expressed as percent of total conductance change, are not significantly changed in the presence of GBZ (Fig. 1B, right part). Consequently, the E/I ratio is not significantly modified (from 22.3 ± 3 % to 25.3 ± 3 %).

Application of 200 nM GBZ induced a significant decrease of IntgI by 38.8 ± 1.2 % and an increase of IntgE by 56.1 ± 2.2 % (n = 17), compared to control values (Fig. 1C and 1D). Consequently, the E/I ratio was significantly enhanced ($p < 0.001$) from 17.8 % / 82.2 % to 38.4 % / 61.6 % in the presence of 200 nM GBZ (Fig. 1D).

Effects of the over-activation of $GABA_A$ receptors on the E/I balance

We next over-stimulated the GABAergic system by perfusing neurons with 4,5,6,7 tetrahydroisoxazolo[5,4-*c*]pyridine-3-ol (THIP), an agonist of $GABA_A$ receptors (Drasbek *et al.*, 2007).

For a given concentration of agonist (10 μM), the amplitude of the current elicited by THIP is higher than that elicited by GABA (data not shown). This indicates that THIP, compared to GABA, is a better agonist of $GABA_A$ receptors, as previously reported (Cope *et al.*, 2005; Drasbek & Jensen, 2006; Liang *et al.*, 2006).

A low concentration of THIP (200 nM) did not affect current responses to layer 2/3 stimulation, as well as global conductance change and its excitatory and inhibitory components (Fig. 2A and 2B). The statistical analysis of the neuronal population (n = 20) shows that the total, excitatory and inhibitory conductance changes were not significantly modified ($p > 0.05$, n = 20). Under these conditions, the E/I ratio remains unchanged (Fig. 2B).

In the presence of 10 μM THIP, the current responses and the total, excitatory and inhibitory conductance changes were decreased (Fig. 2C). This observation was confirmed by the statistical analysis of the neuronal population (n = 24, Fig. 2D). IntgT was decreased from 446.8 ± 82.7 a.u. for the control to 267.6 ± 50.9 a.u. in the presence of THIP, IntgE from 65.2

± 11.2 a.u. to 56.3 ± 11.9 a.u. and IntgI from 381.6 ± 73.6 a.u. to 211.3 ± 42.3 a.u.. Excitatory conductance change, expressed as percent of total conductance change, was significantly increased from 16.9 ± 2.0 % for control to 22.8 ± 2.4 % in the presence of THIP, and the percentage of inhibition was significantly decreased from 83.1 ± 2.0 % to 77.2 ± 2.4 % (Fig. 2D). Consequently, the E/I ratio was slightly but significantly increased by 5.9 % ($p < 0.01$, t-test, $n = 24$).

Homeostatic potentiation induced by application of a HFS protocol in layer 2/3

We previously described a homeostatic potentiation of excitatory and inhibitory inputs on layer 5 pyramidal neurons by application of a HFS protocol in layer 2/3. Marked increases of global, excitatory and inhibitory conductance changes were observed (Le Roux *et al.*, 2006). Similar results were obtained in a new series of experiments (Fig. 3A). Statistical analysis of the global population ($n = 19$, Fig. 3B) shows that the total conductance change is increased by 50 %, due to parallel increases in excitatory and inhibitory conductance changes (Fig. 3C) lasting for one hour. This results in an unchanged E/I ratio.

Lack of time-dependent effects of THIP and GBZ on the E/I balance

Our aim was to determine the involvement of $GABA_A$ synaptic drive in the regulation of the cortical activity and the homeostatic potentiation that occurred after the application of an HFS protocol in layer 2/3. To be confident that possible long lasting changes of the excitatory and inhibitory conductances resulted from the HFS stimulation, and not to a time-dependent effect of the drugs, we determined the E/I balance in the presence of THIP or GBZ, for one hour without application of HFS stimulation.

After a first 20 min recording in the presence of 10 µM THIP, the HFS protocol was omitted and recordings were performed 15, 30, 45 and 60 min later. Representative current recordings

are shown in figure 4A with the corresponding analysis of the total conductance change and of its excitatory and inhibitory components. No time dependent effect of THIP appeared. Moreover, the statistical analysis of the neuronal population (n=5, Figure 4B) shows that the E/I balance did not further change with time and was equal to the value obtained on figure 2D.

The same experimental protocol was applied in the presence of 200nM GBZ. Current recordings were unchanged (not shown) and the statistical analysis of the neuronal population (n=5, Figure 4C) revealed the lack of significant time-dependent effect of GBZ on the E/I balance for one hour.

Potentiation of excitatory and inhibitory inputs induced by HFS protocol is prevented by the blockade of $GABA_A$ receptors

Performing a HFS protocol in the presence of 30 nM GBZ induced a time-dependent depression of IntgT and IntgI (Fig. 5A and 5B). 60 min after application of the HFS protocol, IntgT and IntgI were decreased by 34.1 ± 8.1 % and 39.9 ± 5.9 % (n = 13), whereas IntgE remained almost stable. After application of HFS protocol, the E/I ratio was significantly increased ($p < 0.01$, t-test) from 25.9 % / 74.1 % to 36.1 % / 63.9 % by GBZ (Fig. 5C).

Performing a HFS protocol in the presence of 200 nM GBZ produced a marked depression of IntgT and IntgI (Fig. 5D and 5E). 60 min after application of the HFS protocol, excitation was increased by 33 % while inhibition was decreased by the same ratio (n = 15, Fig. 5F) leading to an increased E/I ratio.

Potentiation of excitatory and inhibitory inputs induced by HFS protocol is prevented by the over-activation of $GABA_A$ receptors

Application of a HFS protocol in the presence of 200 nM THIP induced, after 15 min, a sustained depression of the integrals of total as well as of inhibitory and excitatory conductance changes (Fig. 6A for representative recordings and Fig. 6B for statistical analysis of the global population, n = 18). IntgE, when expressed as percent of IntgT, was increased by 6 % while IntgI was decreased by 6 % after 60 min (Fig. 6C). This resulted in a slight increase of the E/I ratio after HFS application.

In the presence of 10 μM THIP, application of a HFS protocol in layer 2/3 failed to potentiate excitatory and inhibitory conductance changes. On the contrary, a time dependent depression of these conductance changes was observed (Fig. 6D for representative recordings and Fig. 6E for the statistical analysis of the global population, n = 12). 60 min after HFS application, relative conductance changes of IntgE and IntgI (compared to control before HFS protocol) were significantly decreased by about 20 % ($p < 0.05$) and 35 % ($p < 0.001$), respectively. The more important depression of inhibition (expressed as percent of total conductance change) than that of excitation (Fig. 6F) resulted in a significant enhancement of the E/I ratio by 4 % ($p < 0.01$, t-test).

These results show that whatever the concentration of THIP used, HFS protocol fails to induce parallel potentiations of excitatory and inhibitory inputs but induces depressions of these inputs on layer 5 pyramidal neurons. Moreover, the E/I balance was increased indicating that the homeostatic control of plasticity changes (potentiation or depression) was lost.

Interactions between excitatory and inhibitory circuits and their plasticity

The plasticity observed in this phenomenon can depend on modifications of the strength of synapses located either in neuronal circuits upstream layer 5 pyramidal neurons, activated by the stimulation applied in layer 2/3 or on the layer 5 pyramidal neuron itself. The blockade of

excitation with 50 μM CNQX (the selective inhibitor of AMPA receptors) suppressed the excitatory conductance change of the response (Fig. 7A). Under this condition, a reduction by 90 % of the inhibitory conductance change (91.3 % ± 4.8 %, n = 6) was observed indicating that inhibitory afferents recruited by the electrical stimulation in layer 2/3 is mainly disynaptic (inhibitory interneurons activated by afferent glutamatergic neurons). This result suggests that long term potentiation of inhibition may be due to the potentiation of excitatory synapses on inhibitory interneurons.

In the presence of 10 μM bicuculline (the selective blocker of GABAergic receptors), the inhibitory component of the response was abolished and the excitatory component was decreased by 60 % (Fig. 7B). This surprising result indicates that the strength of excitatory inputs received by a layer 5 pyramidal neuron following stimulation in layer 2/3 also partly depends on functional inhibition in the neuronal network.

Discussion

Our data show that a HFS protocol applied to layer 2/3 induces a homeostatic potentiation of excitatory and inhibitory inputs on layer 5 pyramidal neurons leading to an unchanged E/I ratio, provided GABAergic receptors are functional. The blockade or the over-activation of these receptors induces the loss of the E/I balance control and prevents the induction of homeostatic potentiation. Although our results indicate that it remains difficult to finely modulate $GABA_A$ receptors activation, it appears that inhibition is closely related to the excitation processes and those interactions between excitation and inhibition mainly underlie the regulation of cortical networks activity. Since the E/I balance mainly refers to integrative properties of the apical dendrite of layer 5 pyramidal neurons, our results can be discussed first at the level of presynaptic entries on the pyramidal neuron in order to question local modulatory effects of the drugs on presynaptic terminals and second at the level of the cortical organization because homeostatic potentiation of excitation and inhibition was prevented.

Presynaptic modulation of GABA release

Besides inhibitory connections of interneurons on the distal part of apical dendrites of layer 5 pyramidal neurons, projections of interneurons on the proximal part of the apical dendrite *i.e.* on cellular *loci* where a direct modulation of shunting inhibition will be efficient (Wells *et al.,* 2000) is further substantiated by changes of shunting inhibition following HFS protocol in layer 2/3 that have already been reported (Le Roux *et al.,* 2006). Double bouquet cells and bipolar cells which have their soma located in layer 2/3 and axons that project on the apical dendrites of layer 5 pyramidal neurons (Markram *et al.,* 2004), can mainly be involved in these inhibitory afferent inputs. Therefore, the activation or the blockade of presynaptic GABA receptors might change inhibitory inputs and shunting inhibition leading to the loss of

the E/I balance in our experiments. However, it has been reported that THIP does not act on the release of GABA in rat cerebral cortex (Maurin, 1988) and that the blockade of GABA receptors with bicuculline facilitated, inhibited or had no effect on GABA release (Arbilla *et al.*, 1979; Kuryiama *et al.*, 1984; Lockerbie & Gordon-Weeks, 1985). Moreover, it appears recently that presynaptic enhancement of GABA release with GBZ might be efficient in rat juvenile cerebellum but disappear in P15 old rats (Trigo *et al.*, 2007) *i.e.* before the developmental stage (P17-P20) that we used for our experiments. From these observations, presynaptic modulatory effects of THIP or GBZ on GABA release appear not very likely.

Recurrent organization through cortical layers

The neocortex is critical for sensation, perception, behavior and cognition. These functions are ensured by the cortical network. Thus the regulation of network activity which depends on excitatory and inhibitory stimuli received must be closely regulated, and maintaining a balance between excitation and inhibition is a dynamic process. In the cortex, changes in excitation are rapidly countered by changes in synaptic inhibition within several primary sensory areas (Anderson *et al.*, 2000; Shu *et al.*, 2003; Wehr & Zador, 2003; Wilent & Contreras, 2004; Gabernet *et al.*, 2005; Haider *et al.*, 2006; Le Roux *et al.*, 2006). These compensatory changes underlie the phenomenon of homeostatic plasticity which ensures that modification of the strength of one component is compensated by coordinated changes of the other (Davis & Bezprozvanny, 2001; Turrigiano & Nelson, 2004) resulting in an unchanged E/I ratio (Le Roux *et al.*, 2006). However, the cellular mechanisms that ensure this balancing are poorly understood. Recurrent inhibitory circuits seem to be well suited to provide this dynamic regulation (Douglas & Martin, 1991; Shu *et al.*, 2003; Pouille & Scanziani, 2004; Maffei *et al.*, 2004; Le Roux *et al.*, 2006). The main hypothesis concerning the mechanisms of this regulation is based on the recurrent organization of the cortex that produces a robust

feedforward inhibition in response to thalamocortical entries (Agmon & Connors, 1992; Gil & Amitai, 1996; Beierlein *et al.,* 2003; Gabernet *et al.,* 2005; Inoue & Imoto, 2006; Sun *et al.,* 2006). Moreover, recent data suggest a prominent role of feedforward inhibition in the cortex, to strongly control excitation (Ren *et al.,* 2007; Cruikshank *et al.,* 2007) as well.

Among the different schemes for logical operations performed by interneurons in cortical layers (Kullmann & Lamsa, 2007), our experiments are in favour of disynaptic inhibition following the electrical stimulation in layer 2/3. Indeed, 90% of inhibition on layer 5 pyramidal neurons is activated by afferent glutamatergic neurons. Morphological observations are in agreement with this functional approach because layer 5 pyramidal neurons receive inputs both from other layer 5 pyramidal neurons on their proximal basal dendrites (Markram *et al.,* 1997, Silberberg & Markram, 2007) and from layer 2/3 neurons (Thomson & Bannister, 1998), especially from interneurons that project onto the proximal part of apical dendrites (Cipolloni *et al.,* 1998; Bannister, 2005). Since, we showed that the blockade of inhibition produces a 60% decrease of excitation on the layer 5 pyramidal neuron, a recurrent connectivity between layer 5 pyramidal neurons and layer 2/3 neurons is relevant. Chandelier cells in layer 2/3 can recruit pyramidal neurons through specialized $GABA_A$ receptor located on the axonal part of the pyramidal neurons and driving depolarizing signals (Szabadics *et al.,* 2006). Then, similar to the disynaptic inhibition abolished by CNQX, the reduction of the excitatory component in the presence of bicuculline can be due to the blockade of disynaptic recruitment of pyramidal cells by GABAergic chandelier cells. Such a network organization can explain why interneurons which composed 20 % of the cortical neurons account for 80 % in the E/I balance. This idea is further substantiated by recent data indicating that activity in one pyramidal cell evokes inhibition in another pyramidal cell (Kapfer *et al.,* 2007; Silberberg & Markram, 2007). Excitatory activity in layer 2/3 of the somatosensory cortex is also shown to specifically recruit a recurrent inhibitory circuit involving somatostatin interneurons

located in layers 2/3 and 5. Through this circuit a single pyramidal cell can cause inhibition of almost 40 % of its neighbors (Kapfer *et al.,* 2007).

$GABA_A$ receptors and E/I balance of layer 5 pyramidal neurons

Low concentrations of THIP or GBZ did not change the E/I balance. Thus, it can be assumed that regulatory mechanisms controlling the E/I balance are potent enough to compensate for weak changes in cortical inhibitory activity.

On the contrary, the effective blockade or the over-activation of $GABA_A$ receptors led to changes in the strength of the inhibitory synaptic inputs. The blockade of $GABA_A$ receptors did not change the strength of excitatory inputs but decreased inhibitory inputs on layer 5 pyramidal neurons, leading to an important enhancement of the E/I balance. It has been shown that an E/I balance equal to 20/80 % corresponds to a set-point control keeping the layer 5 pyramidal neurons and cortical networks within functional range (Le Roux *et al.,* 2006). It requires at least recurrent connectivity between excitatory and inhibitory neuronal circuits and this condition is discussed above. Taking into account that 200 nM GBZ markedly increased the E/I balance, we conclude that this blockage of GABA receptors probably disrupt recurrent interactions between excitatory and inhibitory neuronal networks. Conversely, the use of a $GABA_A$ agonist decreased E and I resulting in a weak enhancement (by 5.9 %) of the E/I balance. Thus one can postulate that compensatory interactions between excitatory and inhibitory networks appear to remain functional during $GABA_A$ receptor stimulation.

It is important to note that in the presence of a $GABA_A$ receptor agonist, the inhibitory conductance change was decreased. This data can be explained by a switch of GABAergic responses following prolonged $GABA_A$ receptor activation from a hyperpolarizing to a depolarizing response as observed in mature cortical neurons (Lambert *et al.,* 1991; Staley *et*

al., 1995; Kaila *et al.*, 1997; Taira *et al.*, 1997; Staley & Proctor, 1999; Gulledge & Stuart, 2003). This is likely due to a positive shift of the reversal potential of Cl^- current as the result of Cl^- accumulation in neurons (Staley *et al.*, 1995; Backus *et al.*, 1998; Dallwig *et al.*, 1999; Frech *et al.*, 1999; Jedlicka & Backus, 2006). Prolonged activation of $GABA_A$ receptor with THIP can also desensitize the receptors and consequently lead to a decrease in the strength of inhibitory inputs on layer 5 pyramidal neurons.

$GABA_A$ receptors and homeostatic plasticity

The HFS protocol induced a slight increase of the E/I balance when $GABA_A$ receptors were activated and a strong enhancement of the E/I balance (70% / 30%) in the presence of GBZ. The results indicate that impairing the GABAergic transmission suppress the coordinated processes assuming homeostatic potentiation of excitatory and inhibitory inputs on layer 5 pyramidal neuron (Le Roux *et al.*, 2006) and lead to a LTD-like effect instead of the expected LTP. However, taking into account the extent of changes in the E/I balance, it can be assumed that the over-activation of $GABA_A$ receptors prevent the homeostatic control of excitatory and inhibitory neuronal circuits while their blockade can largely deregulate the mechanisms of the homeostatic plasticity in neuronal networks. This supports the idea that inhibitory interneurons (as already discussed above) are critical for recurrent interactions underlying normal plasticity in cortical networks.

Plasticity of excitatory and inhibitory cortico-cortical inputs

The concept of homeostatic plasticity is based on interactions and coordination between excitatory and inhibitory neuronal circuits. Recent data indicate that inhibition increases linearly with the amount of excitation received by cortical neurons (Anderson *et al.*, 2000; Wehr & Zador, 2003; Wilent & Contreras, 2004**).** Adjustment of excitatory and inhibitory

synaptic strengths have been observed in experiments of visual deprivation in which changes in excitatory synaptic drive induce compensatory changes in the inhibitory synaptic drive to maintain stable levels of activity in the developing visual cortex (Turrigiano, 1999; Maffei *et al.*, 2004, 2006). Our previous experiments indicate that simultaneous compensatory potentiations of excitation and inhibition are induced after application of a HFS protocol (Le Roux *et al.*, 2006). These results raise the question of the coordinated induction of the plasticity of excitatory and inhibitory synapses. Because the inhibition is mainly disynaptic, it can be proposed that, the feedforward inhibitory pathway involves at least upstream excitatory fibers originating from layer 5 which synapse on layer 2/3 interneurons. Such a scheme was also described in the hippocampus where NMDA-receptor-dependent LTP in interneurons mainly depends on the feedforward inhibitory pathway (Lamsa *et al.*, 2005) and in the retinotectal system (Liu *et al.*, 2007). These results indicate that GABAergic plasticity can be guided by glutamatergic transmission and that inhibitory plasticity can mainly occur in parallel with excitatory plasticity. This fits also with the classical paradigm assuming that in the cortex inhibitory connections preserve network stability by preventing runaway excitation (Tsodyks *et al.*, 1997). It needs simultaneous strengthening of disynaptic inhibition that may act to optimize the information-storage capacity of the network by preventing excessive excitation of the output neurons.

Acknowledgments The authors thank Dr. E. Benoit and Dr. S. O'Regan for critical reading of the manuscript.

References

Abraham, W.C. & Huggett, A. (1997) Induction and reversal of long-term potentiation by repeated high-frequency stimulation in rat hippocampal slices. *Hippocampus* 7, 137-145.

Agmon, A. & Connors, B.W. (1992) Correlation between intrinsic firing patterns and thalamocortical synaptic responses of neurons in mouse barrel cortex. *J. Neurosci.* **12**, 319-329.

Anderson, J.S., Carandini, M. & Ferster, D. (2000) Orientation tuning of input conductance, excitation, and inhibition in cat primary visual cortex. *J. Neurophysiol.* **84**, 909-926.

Arbilla, S., Kamal, L. & Langer, S.Z. (1979) Presynaptic GABA autoreceptors on GABAergic nerve endings of the rat substantia nigra. *Eur. J. Pharmacol.* **57**, 211-217.

Backus, K.H., Deitmer, J.W. & Friauf, E. (1998) Glycine-activated currents are changed by coincident membrane depolarization in developing rat auditory brainstem neurones. *J. Physiol.* **507** (Pt 3), 783-794.

Bannister, A.P. (2005) Inter- and intra-laminar connections of pyramidal cells in the neocortex. *Neurosci. Res.* **53**, 95-103.

Beierlein, M., Gibson, J.R. & Connors, B.W. (2003) Two dynamically distinct inhibitory networks in layer 4 of the neocortex. *J. Neurophysiol.* **90**, 2987-3000.

Borg-Graham, L.J., Monier, C. & Fregnac, Y. (1998) Visual input evokes transient and strong shunting inhibition in visual cortical neurons. *Nature* **393**, 369-373.

Bradler, J.E. & Barrioneuvo, G. (1989) Long-term potentiation in hippocampal CA3 neurons: tetanized input regulates heterosynaptic efficacy. *Synapse* **4**, 132-142.

Caillard, O., Ben-Ari, Y. & Gaiarsa, J.L. (1999a) Long-term potentiation of GABAergic synaptic transmission in neonatal rat hippocampus. *J. Physiol.* **18** (Pt 1), 109-119.

Caillard, O., Ben-Ari, Y. & Gaiarsa, J.L. (1999b) Mechanisms of induction and expression of long-term depression at GABAergic synapses in the neonatal rat hippocampus. *J. Neurosci.* **19**, 7568-7577.

Cipolloni, P.B., Kimerer, L., Weintraub, N.D., Smith, D.V. & Keller, A. (1998) Distribution of inhibitory synapses on the somata of pyramidal neurons in cat motor cortex. *Somatosens. Mot. Res.* **15**, 276-286.

Cline, H. (2005) Synaptogenesis: a balancing act between excitation and inhibition. *Curr. Biol.* **15**, R203-205.

Cope, D.W., Hughes, S.W. & Crunelli, V. (2005) GABAA receptor-mediated tonic inhibition in thalamic neurons. *J. Neurosci.* **25**, 11553-11563.

Cruikshank, S.J., Lewis, T.J. & Connors, B.W. (2007) Synaptic basis for intense thalamocortical activation of feedforward inhibitory cells in neocortex. *Nat. Neurosci.* **10**, 462-468.

Dallwig, R., Deitmer, J.W. & Backus, K.H. (1999) On the mechanism of GABA-induced currents in cultured rat cortical neurons. *Pflugers Arch.* **437**, 289-297.

Davis, G.W. & Bezprozvanny, I. (2001) Maintaining the stability of neural function: a homeostatic hypothesis. *Annu. Rev. Physiol.* **63**, 847-869.

Davis, G.W. (2006) Homeostatic control of neural activity: from phenomenology to molecular design. *Annu. Rev. Neurosc.* **29**, 307-323.

Douglas, R.J. & Martin, K.A. (1991) A functional microcircuit for cat visual cortex. *J. Physiol.* **440**, 735-769.

Drasbek, K.R., Hoestgaard-Jensen, K. & Jensen, K. (2007) Modulation of extrasynaptic THIP conductances by GABAA receptor modulators in mouse neocortex. *J Neurophysiol.* **97**, 2293-2300.

Drasbek, K.R. & Jensen, K. (2006) THIP, a Hypnotic and Antinociceptive Drug, Enhances an Extrasynaptic GABAA Receptor-mediated Conductance in Mouse Neocortex. *Cereb. Cortex* **16**, 1134-1141.

Erickson, J.D., De Gois, S., Varoqui, H., Schafer, M.K. & Weihe, E. (2006) Activity-dependent regulation of vesicular glutamate and GABA transporters: a means to scale quantal size. *Neurochem. Int.* **48**, 643-649.

Frech, M.J., Deitmer, J.W. & Backus, K.H. (1999) Intracellular chloride and calcium transients evoked by gamma-aminobutyric acid and glycine in neurons of the rat inferior colliculus. *J. Neurobiol.* **40**, 386-396.

Freund, T.F. (2003) Interneuron Diversity series: Rhythm and mood in perisomatic inhibition. *Trends Neurosci.* **26**, 489-495.

Freund, T.F. & Gulyas, A.I. (1997) Inhibitory control of GABAergic interneurons in the hippocampus. *Can. J. Physiol. Pharmacol.* **75**, 479-487.

Gabernet, L., Jadhav, S.P., Feldman, D.E., Carandini, M. & Scanziani, M. (2005) Somatosensory integration controlled by dynamic thalamocortical feed-forward inhibition. *Neuron* **48**, 315-327.

Gaiarsa, J.L., Caillard, O. & Ben-Ari, Y. (2002) Long-term plasticity at GABAergic and glycinergic synapses: mechanisms and functional significance. *Trends Neurosci.* **25**, 564-570.

Gil, Z. & Amitai, Y. (1996) Properties of convergent thalamocortical and intracortical synaptic potentials in single neurons of neocortex. *J. Neurosci.* **16**, 6567-6578.

Gulledge, A.T. & Stuart, G.J. (2003) Action potential initiation and propagation in layer 5 pyramidal neurons of the rat prefrontal cortex: absence of dopamine modulation. *J. Neurosci.* **23**, 11363-11372.

Haider, B., Duque, A., Hasenstaub, A.R. & McCormick, D.A. (2006) Neocortical network activity in vivo is generated through a dynamic balance of excitation and inhibition. *J. Neurosci.* **26**, 4535-4545.

Higley, M.J. & Contreras, D. (2006) Balanced excitation and inhibition determine spike timing during frequency adaptation. *J. Neurosci.* **26**, 448-457.

Inoue, T. & Imoto, K. (2006) Feedforward inhibitory connections from multiple thalamic cells to multiple regular-spiking cells in layer 4 of the somatosensory cortex. *J. Neurophysiol.* **96**, 1746-1754.

Jedlicka, P. & Backus, K.H. (2006) Inhibitory transmission, activity-dependent ionic changes and neuronal network oscillations. *Physiol. Res.* **55**, 139-149.

Kaila, K., Lamsa, K., Smirnov, S., Taira, T. & Voipio, J. (1997) Long-lasting GABA-mediated depolarization evoked by high-frequency stimulation in pyramidal neurons of rat hippocampal slice is attributable to a network-driven, bicarbonate-dependent K+ transient. *J. Neurosci.* **17**, 7662-7672.

Kapfer, C., Glickfeld, L.L., Atallah, B.V. & Scanziani, M. (2007) Supralinear increase of recurrent inhibition during sparse activity in the somatosensory cortex. *Nat. Neurosci.* **10**, 743-753.

Kullmann, D.M. & Lamsa, K.P. (2007) Long-term synaptic plasticity in hippocampal interneurons. *Nat. Rev. Neurosci.* **8**, 687-699.

Kuriyama, K., Kanmori, K., Taguchi, J. & Yoneda, Y. (1984) Sress-induced enhancement of suppression of (^{3}H)GABA release from striatal slices by presynaptic autoreceptor. *J. Neurochem.* **42**, 943-950.

Lambert, N.A., Borroni, A.M., Grover, L.M. & Teyler, T.J. (1991) Hyperpolarizing and depolarizing GABAA receptor-mediated dendritic inhibition in area CA1 of the rat hippocampus. *J. Neurophysiol.* **66**, 1538-1548.

Lamsa, K., Heeroma, J.H. & Kullmann, D.M. (2005) Hebbian LTP in feed-forward inhibitory interneurons and the temporal fidelity of input discrimination. *Nat. Neurosci.* **8**, 916-924.

Le Roux, N., Amar, M., Baux, G. & Fossier, P. (2006) Homeostatic control of the excitation-inhibition balance in cortical layer 5 pyramidal neurons. *Eur. J. Neurosci.* **24**, 3507-3518.

Le Roux, N., Amar, M., Moreau, A. & Fossier, P. (2007) Involvement of NR2A- or NR2B-containing N-methyl-D-aspartate receptors in the potentiation of cortical layer 5 pyramidal neurone inputs depends on the developmental stage. *Eur. J. Neurosci.* **26**, 289-301.

Liang, J., Zhang, N., Cagetti, E., Houser, C.R., Olsen, R.W. & Spigelman, I. (2006) Chronic intermittent ethanol-induced switch of ethanol actions from extrasynaptic to synaptic hippocampal GABAA receptors. *J. Neurosci.* **26**, 1749-1758.

Liu, Y., Zhang, L.I. & Tao, H.W. (2007) Heterosynaptic scaling of developing GABAergic synapses: dependence on glutamatergic input and developmental stage. *J. Neurosci.* **27**, 5301-5312.

Lockerbie, R.O. & Gordon-Weeks, P.R. (1985) Gamma-aminobutyric $acid_A$ ($GABA_A$) receptors modulate (^{3}H)GABA release from isolated neuronal growth cones in the rat. *Neurosci. Lett.* **55**, 273-277.

Lu, Y.M., Mansuy, I.M., Kandel, E.R. & Roder, J. (2000) Calcineurin-mediated LTD of GABAergic inhibition underlies the increased excitability of CA1 neurons associated with LTP. *Neuron* **26**, 197-205.

Maffei, A., Nelson, S.B., Turrigiano, G.G. (2004) Selective configuration of layer 4 visual cortical circuitry by visual deprivation. *Nat. Neurosci.* **7**, 1353-1359.

Maffei, A., Nataraj, K., Nelson, S.B. & Turrigiano, G.G. (2006) Potentiation of cortical inhibition by visual deprivation. *Nature* **443**, 81-84.

Marder, E. & Prinz, A.A. (2002) Modeling stability in neuron and network function: the role of activity in homeostasis. *Bioessays* **24**, 1145-1154.

Markram, H., Lubke, J., Frotscher, M., Roth, A. & Sakmann, B. (1997) Physiology and anatomy of synaptic connections between thick tufted pyramidal neurones in the developing rat neocortex. *J Physiol* **500** (Pt 2), 409-440.

Markram, H., Toledo-Rodriguez, M., Wang, Y., Gupta, A., Silberberg, G. & Wu, C. (2004) Interneurons of the neocortical inhibitory system. *Nat. Rev. Neurosci.* **5**, 793-807.

Maurin, Y. (1988) Paradoxical antagonism by bicuculline of the inhibition by baclofen of the electrically evoked release of [3H]GABA from rat cerebral cortex slices. *Eur. J. Pharmacol.* **155**, 219-227.

McBain, C.J. & Fisahn, A. (2001) Interneurons unbound. *Nat. Rev. Neurosci.* **2**, 11-23.

Monier, C., Chavane, F., Baudot, P., Graham, L.J. & Fregnac, Y. (2003) Orientation and direction selectivity of synaptic inputs in visual cortical neurons: a diversity of combinations produces spike tuning. *Neuron* **37**, 663-680.

Monier, C., Fournier, J. & Fregnac, F. (2008) In vitro and in vivo measures of evoked excitatory and inhibitory conductance dynamics in sensory cortices, *J Neurosci Methods* **169**, 323-365.

Nugent, F.S., Penick, E.C. & Kauer, J.A. (2007) Opioids block long-term potentiation of inhibitory synapses. *Nature* **446**, 1086-1090.

Peters, A. & Kara, D.A. (1985) The neuronal composition of area 17 of rat visual cortex. II. The nonpyramidal cells. *J. Comp. Neurol.* **234**, 242-263.

Pouille, F. & Scanziani, M. (2004) Routing of spike series by dynamic circuits in the hippocampus. *Nature* **429**, 717-723.

Ren, M., Yoshimura, Y., Takada, N., Horibe, S. & Komatsu, Y. (2007) Specialized inhibitory synaptic actions between nearby neocortical pyramidal neurons. *Science* **316**, 758-761.

Szabadics, J., Varga, C., Molnar, G., Olah, S., Barzo, P. & Tamas, G. (2006) Excitatory effect of GABAergic axo-axonic cells in cortical microcircuits. *Science* **13**, 233-235.

Shu, Y., Hasenstaub, A. & McCormick, D.A. (2003) Turning on and off recurrent balanced cortical activity. *Nature* **423**, 288-293.

Silberberg, G. & Markram, H. (2007) Disynaptic inhibition between neocortical pyramidal cells mediated by Martinotti cells. *Neuron* **53**, 735-746.

Staley, K.J. & Proctor, W.R. (1999) Modulation of mammalian dendritic GABA(A) receptor function by the kinetics of Cl- and HCO3- transport. *J. Physiol.* **519** Pt 3, 693-712.

Staley K.J., Soldo B.L. & Proctor, W.R. (1995) Ionic mechanisms of neuronal excitation by inhibitory GABAA receptors. *Science* **269**, 977-981.

Steele, P.M. & Mauk, M.D. (1999) Inhibitory control of LTP and LTD: stability of synapse strength. *J. Neurophysiol.* **81**, 1559-1566.

Sun, Q.Q., Huguenard, J.R. & Prince, D.A. (2006) Barrel cortex microcircuits: thalamocortical feedforward inhibition in spiny stellate cells is mediated by a small number of fast-spiking interneurons. *J. Neurosci.* **26**, 1219-1230.

Taira, T., Lamsa, K. & Kaila, K. (1997) Posttetanic excitation mediated by GABA(A) receptors in rat CA1 pyramidal neurons. *J. Neurophysiol.* **77**, 2213-2218.

Tamas, G., Buhl, E.H., Lorincz, A. & Somogyi, P. (2000) Proximally targeted GABAergic synapses and gap junctions synchronize cortical interneurons. *Nat. Neurosci.* **3**, 366-371.

Thomson, A.M. & Bannister, A.P. (1998) Postsynaptic pyramidal target selection by descending layer III pyramidal axons: dual intracellular recordings and biocytin filling in slices of rat neocortex. *Neuroscience* **84**, 669-683.

Trigo, F.F., Chat, M. & Marty, A. (2007) Enhancement of GABA release through endogenous activation of axonal GABAA receptors in juvenile cerebellum. *J. Neurosci.* **27**, 12452-12463.

Tsodyks, M.V., Skaggs, W.E., Sejnowski, T.J. & McNaughton, B.L. (1997) Paradoxical effects of external modulation of inhibitory interneurons. *J. Neurosci.* **17**, 4382-4388.

Turrigiano, G.G., Leslie, K.R., Desai, N.S., Rutherford, L.C. & Nelson, S.B. (1998) Activity-dependent scaling of quantal amplitude in neocortical neurons. *Nature* **391**, 892-896.

Turrigiano, G.G. (1999) Homeostatic plasticity in neuronal networks: the more things change, the more they stay the same. *Trends Neurosci.* **22**, 221-227.

Turrigiano, G.G. & Nelson, S.B. (2004) Homeostatic plasticity in the developing nervous system. *Nat. Rev. Neurosci.* **5**, 97-107.

Turrigiano, G.G. (2007) Homeostatic signaling: the positive side of negative feedback. *Curr. Opin. Neurobiol.* **17**, 318-324.

Wehr, M. & Zador, A.M. (2003) Balanced inhibition underlies tuning and sharpens spike timing in auditory cortex. *Nature* **426**, 442-446.

Wells, J.E., Porter, J.T. & Agmon, A. (2000) GABAergic inhibition suppresses paroxysmal network activity in the neonatal rodent hippocampus and neocortex. *J. Neurosci.* **20**, 8822-8830.

Wilent, W.B. & Contreras, D. (2004) Synaptic responses to whisker deflections in rat barrel cortex as a function of cortical layer and stimulus intensity. *J. Neurosci.* **24**, 3985-3998.

Zilberter, Y. (2000) Dendritic release of glutamate suppresses synaptic inhibition of pyramidal neurons in rat neocortex. *J. Physiol.* **528**, 489-496.

Figure 1. Effects of $GABA_A$ receptors blockade on the E/I balance of layer 5 pyramidal neurons.

(**A**) The left column shows a representative recording in control condition and the right column after application of 30 nM GBZ during 20 min. **Upper traces**: current responses of a layer 5 pyramidal neuron to electrical stimulation (black arrow) applied in layer 2/3; holding potentials scaled from – 75 (bottom trace) to – 55 mV (steps equal to 5 mV). **Medium traces**: decomposition of the responses in total conductance change (gT). **Lower traces**: decomposition of gT in excitatory and inhibitory conductance changes (gE, dark grey and gI, light grey). No significant variation of total, excitatory and inhibitory conductance changes were observed.

(**B**) Left part: relative changes (compared to control) of IntgT (black bars), IntgE (dark grey bars) and IntgI (light grey bars), after application of 30 nM GBZ (n = 11). Right part: excitation (black bars) and inhibition (white bars) conductance changes expressed as percents of the total conductance change. The E/I ratio remains unchanged.

(**C**) The left column shows a representative recording in control condition and the right column after application of 200 nM GBZ during 20 min. Legends are identical as in Fig. 1A. In the presence of 200 nM the inward current was increased whereas the outward component was decreased.

(**D**) Left part: relative changes (compared to control) of IntgT (black bars), IntgE (dark grey bars) and IntgI (light grey bars), after application of 200 nM GBZ (n = 17). Right part: excitation (black bars) and inhibition (white bars) conductance changes expressed as percents of the total conductance change in control condition (left, c) and in the presence of GBZ (right). Excitation increased from 17.8 ± 2.5 % of the total conductance change to 38.5 ± 5.0 % and inhibition decreased from 82.2 ± 2.5 % to 61.5 ± 5.0 %. (*** $p<0.001$, ** $p<0.01$ and * $p<0.05$, t-test).

Figure 2. Effects of $GABA_A$ receptors activation on the E/I balance of layer 5 pyramidal neurons.

(**A and C**) Left columns show representative recordings in control condition and right columns after 20 min application of THIP (200 nM or 10 μM, respectively). **Upper traces**: current responses of a layer 5 pyramidal neuron to electrical stimulation (black arrow) applied in layer 2/3; holding potentials scaled from –70 (bottom trace) to –50 mV (steps equal to 5 mV). **Medium traces**: decomposition of the responses in total conductance changes (gT). **Lower traces**: decomposition of gT in excitatory (gE, dark grey) and inhibitory (gI, light grey) conductance changes. Note that the current responses and the conductance changes remain unchanged in the presence of 200 nM THIP (A) whereas they were decreased in the presence of 10 μM THIP (C).

(**B**) The left part shows relative changes (compared to control) of IntgT (black bars), IntgE (dark grey bars) and IntgI (light grey bars), after 200 nM THIP application (n = 20). The right part shows excitation (black bars) and inhibition conductances (white bars) expressed as percents of the total conductance change (c: control). No significant change of excitation and inhibition was observed.

(**D**) Left part: relative changes (compared to control) of IntgT (black bars), IntgE (dark grey bars) and IntgI (light grey bars), after 10 μM THIP application (n = 24). Right part: excitation (black bars) and inhibition conductances (white bars) expressed as percents of the total conductance change (c: control on the left and in the presence of THIP on the right). Excitation was increased from 16.9 ± 2.0 % to 22.8 ± 2.4 % and inhibition was decreased from 83.1 ± 2.0 % to 77.2 ± 2.4 %.

(*** $p<0.001$, ** $p<0.01$ and * $p<0.05$, t-test).

Figure 3. Effects of the application of a HFS protocol in layer 2/3 on the E/I balance of layer 5 pyramidal neurons.

(**A**) The left column shows representative recordings from the statistical analysis of n = 19 experiments in control conditions, the middle column 30 min after application of HFS protocol in layer 2/3 and the right column 60 min after application of HFS. **Upper traces**: current responses of a layer 5 pyramidal neuron to electrical stimulation. Imposed membrane potential ranged for –55 to –75 mV. Note that the amplitude of current responses was increased after HFS application. **Medium traces**: decomposition of the responses in total conductance change (gT). **Lower traces**: decomposition of gT in excitatory and inhibitory conductance changes (gE, dark grey and gI, light grey). Total, excitatory and inhibitory conductance changes were increased after HFS application.

(**B**) Relative changes (compared to control) of IntgT (black bars), IntgE (dark grey bars) and IntgI (light grey bars), after application of HFS protocol in layer 2/3 in control conditions (n = 19). (*** $p<0.001$, ** $p<0.01$ and * $p<0.05$, t-test).

(**C**) Relative contribution of excitation (black) and inhibition (white) conductance changes to the total conductance change, various times (15, 30, 45 and 60 min) after HFS (c:control before HFS protocol).

Figure 4. Lack of time-dependent effect of THIP or GBZ on the E/I balance.

(**A**) Representative recordings and corresponding conductance determinations in the presence of 10 µM THIP applied during one hour after a first 20 min period of application. **Upper traces**: current responses of a representative layer 5 pyramidal neuron to electrical stimulation. Imposed membrane potential ranged for –55 to –75 mV. **Medium traces**: decomposition of the responses in total conductance (gT). **Lower traces**: decomposition of

gT in excitatory and inhibitory conductance (gE, dark grey and gI, light grey). No change in total, inhibitory or excitatory conductance was observed during THIP application.

(**B**) Relative contribution of excitation (black) and inhibition (white) conductance changes to the total conductance change. Recordings were performed 15, 30, 45 or 60 min after a control recording (t = 0) made 20 min after application of 10 µM THIP. Bars represent the ratio between recordings 15, 30, 45 or 60 and the t = 0 control recording. Note that the E/I ratio remained stable.

(**C**) Relative contribution of excitation (black) and inhibition (white) conductance changes to the total conductance change during 60 min in the presence of 200 nM GBZ. Legends are identical than in B. No significant change of the E/I ratio was observed.

Figure 5. Effects of a HFS protocol in the presence of GBZ.

(**A**) The left column shows a representative recording from the statistical analysis of n = 13 experiments in the presence of 30 nM GBZ before HFS application, the middle column 30 min after application of HFS protocol and the right column 60 min after application of HFS in layer 2/3. **Upper traces**: current responses of a layer 5 pyramidal neuron to electrical stimulation. Imposed membrane potential ranged for –55 to –75 mV. The inward current was not modified whereas the outward component was decresed. **Medium traces**: decomposition of the responses in total conductance change (gT). **Lower traces**: decomposition of gT in excitatory and inhibitory conductance changes (gE, dark grey and gI, light grey). The total and inhibitory conductance changes were decreased after HFS application.

(**B**) Relative changes (compared to control) of IntgT (black bars), IntgE (dark grey bars) and IntgI (light grey bars), after HFS protocol in layer 2/3 (n = 14) in the presence of 30 nM GBZ. (*** $p<0.001$, ** $p<0.01$ and * $p<0.05$, t-test).

(**C**) Relative contribution of excitation and inhibition conductance changes to the total conductance change, after application of HFS protocol in the presence of 200 nM GBZ (c: control before HFS protocol). Note that the E/I ratio strongly increased.

(**D-E-F**) Application of HFS protocol in the presence of 200 nM GBZ (n = 14). Legends are identical as in **A-B-C**. The total and inhibitory conductance changes were decreased (**D-E**) and the E/I ratio was increased (**F**).

Figure 6. Effects of a HFS protocol in the presence of THIP.

(**A**) The left column shows a representative recordings from the statistical analysis of n = 18 experiments in the presence of 200 nM THIP before HFS application, the middle column 30 min after application of HFS protocol and the right column 60 min after application of HFS in layer 2/3. **Upper traces**: current responses of a layer 5 pyramidal neuron to electrical stimulation. Imposed membrane potential ranged for –55 to –75 mV. **Medium traces**: decomposition of the responses in total conductance change (gT). **Lower traces**: decomposition of gT in excitatory and inhibitory conductance changes (gE, dark grey and gI, light grey). Total, inhibitory and excitatory conductance changes were decreased after HFS application.

(**B**) Relative changes (compared to control) of IntgT (black bars), IntgE (dark grey bars) and IntgI (light grey bars), after HFS in layer 2/3 (n = 18) in the presence of 200 nM THIP. (*** $p<0.001$, ** $p<0.01$ and * $p<0.05$, t-test).

(**C**) Relative contribution of excitation and inhibition conductance changes to the total conductance change, after HFS in the presence of 200 nM THIP (c:control before HFS protocol). Note that the E/I ratio was increased.

(**D-E-F**) Application of HFS protocol in the presence of 10 μM THIP (n = 16). Legends are identical as in **A-B-C**. Total, excitatory and inhibitory conductance changes were decreased (**D-E**) and the E/I ratio was increased (**F**).

Figure 7. The inhibition recorded in a layer 5 pyramidal neuron to electrical stimulation of layer 2/3 is mainly disynaptic.

Upper traces: current responses obtained after stimulation (arrow) of layers 2/3. Medium traces: decomposition of the responses in global conductance change (gT). Lower traces: decomposition of gT in excitatory and inhibitory conductance changes.

(**A**) Left column: control conditions, right column: after the blockade of glutamatergic receptors by CNQX. Note that in the presence of CNQX, the excitatory component of the response was abolished whereas the inhibitory component was decreased by about 85 %, indicating that inhibition is mainly disynaptic.

(**B**) Left column: control conditions, right column: after the blockade of GABAergic receptors by bicuculline. Note that the inhibitory component was abolished whereas the excitatory component was decreased by about 60 %.

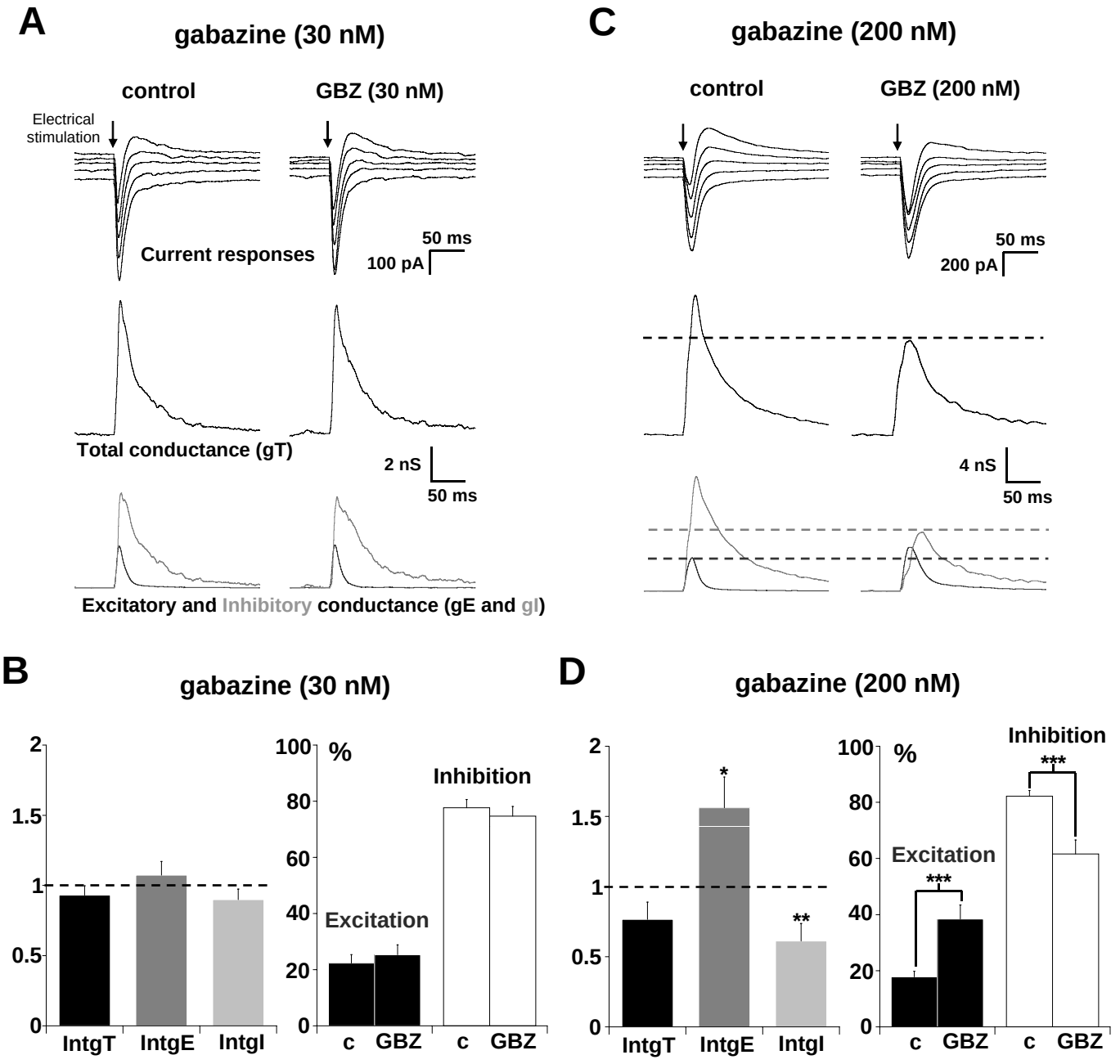
A
gabazine (30 nM)
control
GBZ (30 nM)
Electrical stimulation
Current responses
50 ms
100 pA
Total conductance (gT)
2 nS
50 ms
Excitatory and Inhibitory conductance (gE and gI)
C
gabazine (200 nM)
control
GBZ (200 nM)
50 ms
200 pA
4 nS
50 ms
B
gabazine (30 nM)
IntgT
IntgE
IntgI
%
Inhibition
Excitation
c
GBZ
D
gabazine (200 nM)
*
**
***

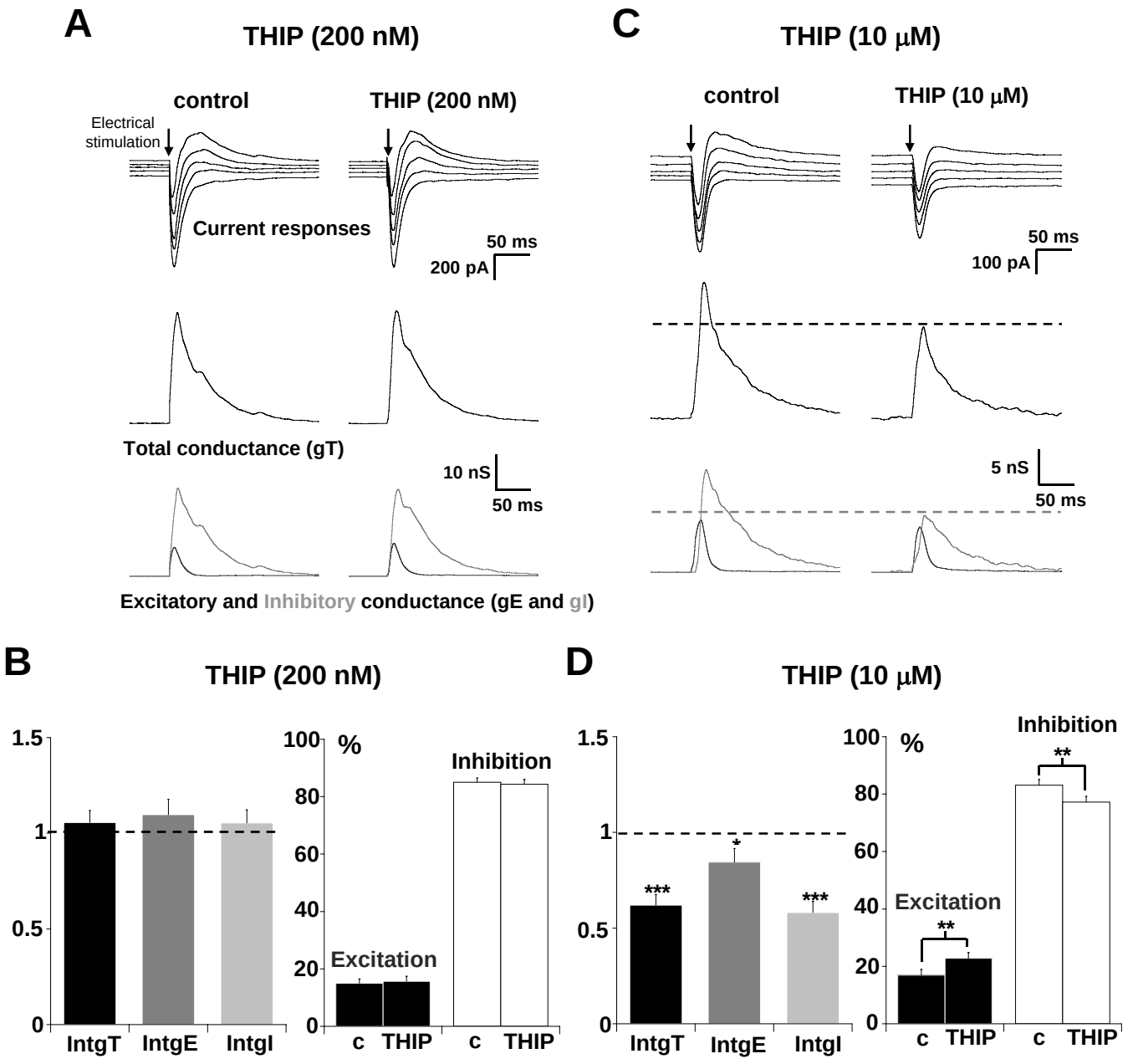
A
THIP (200 nM)
control
THIP (200 nM)
Electrical stimulation
Current responses
50 ms
200 pA
Total conductance (gT)
10 nS
50 ms
Excitatory and Inhibitory conductance (gE and gI)
C
THIP (10 μM)
control
THIP (10 μM)
50 ms
100 pA
5 nS
50 ms
B
THIP (200 nM)
1.5
1
0.5
0
IntgT
IntgE
IntgI
100
%
80
60
40
20
0
Excitation
Inhibition
c
THIP
c
THIP
D
THIP (10 μM)
1.5
1
0.5
0
***
*
***
IntgT
IntgE
IntgI
100
%
80
60
40
20
0
Excitation
**
Inhibition
**
c
THIP
c
THIP

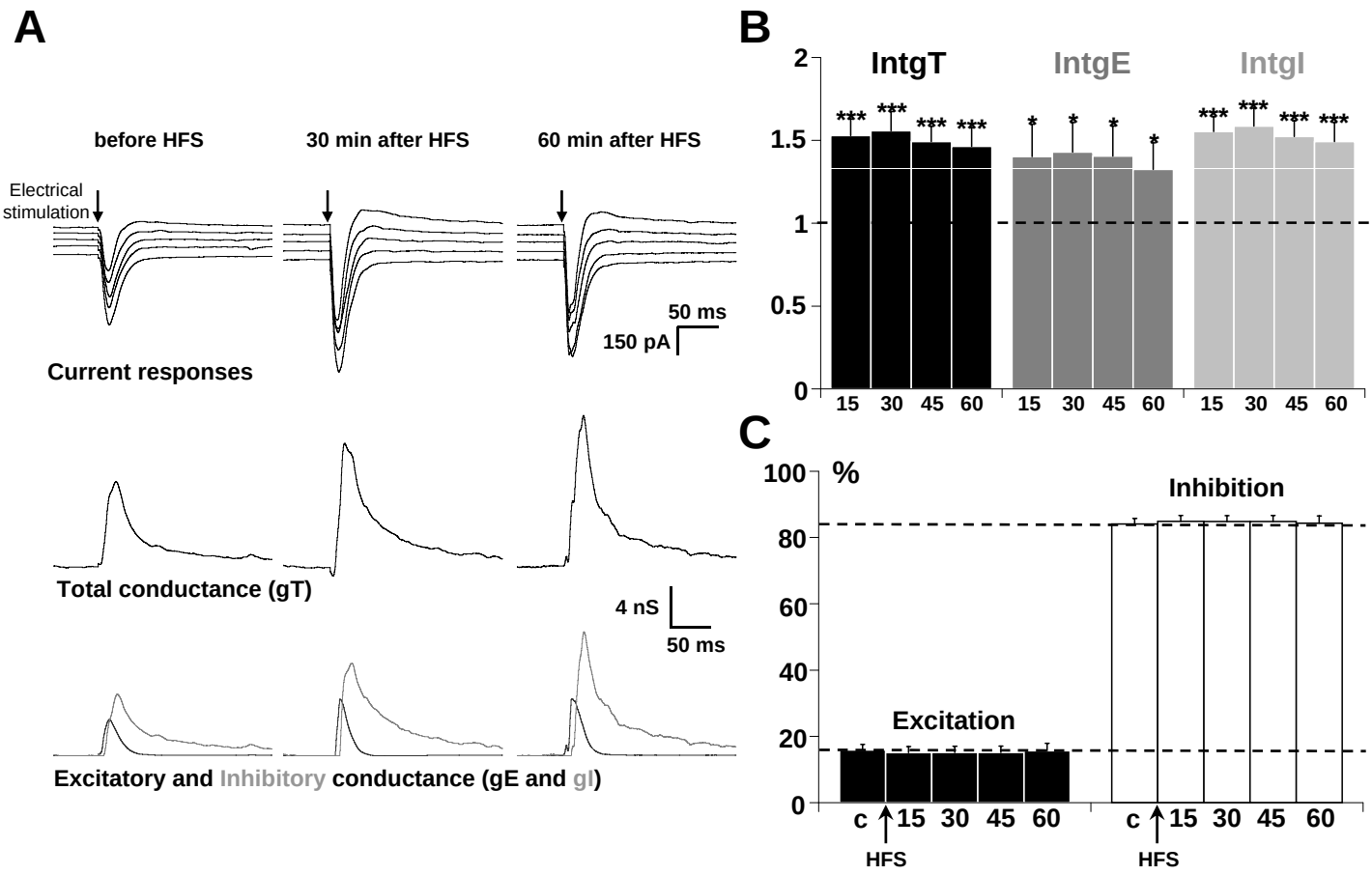
A
before HFS
30 min after HFS
60 min after HFS
Electrical stimulation
50 ms
150 pA
Current responses
Total conductance (gT)
4 nS
50 ms
Excitatory and Inhibitory conductance (gE and gI)
B
IntgT
IntgE
IntgI
2
1.5
1
0.5
0
15 30 45 60
C
100
%
80
60
40
20
0
Inhibition
Excitation
c 15 30 45 60
HFS

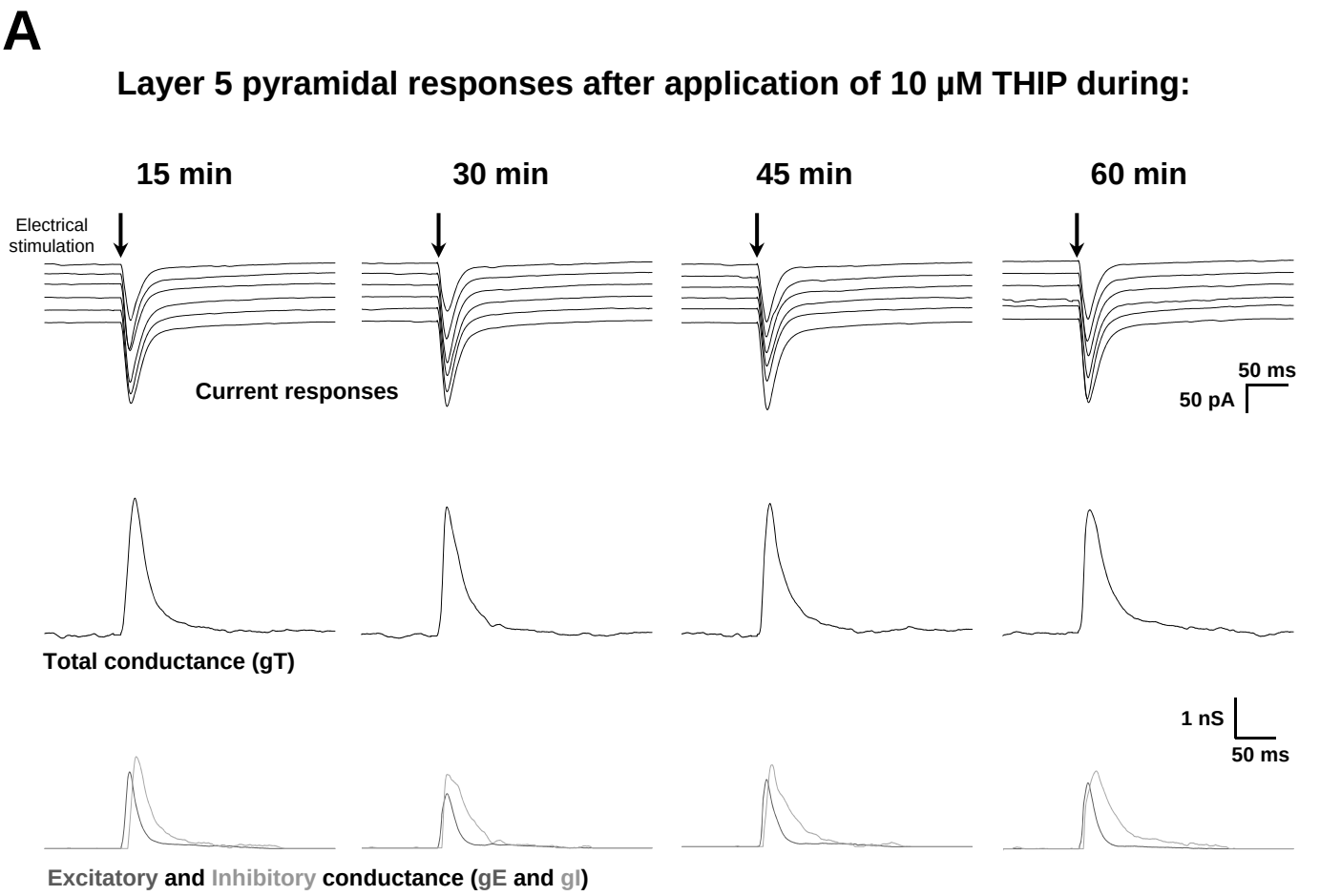
A
Layer 5 pyramidal responses after application of 10 µM THIP during:
15 min
30 min
45 min
60 min
Electrical stimulation
Current responses
50 ms
50 pA
Total conductance (gT)
1 nS
50 ms
Excitatory and Inhibitory conductance (gE and gI)

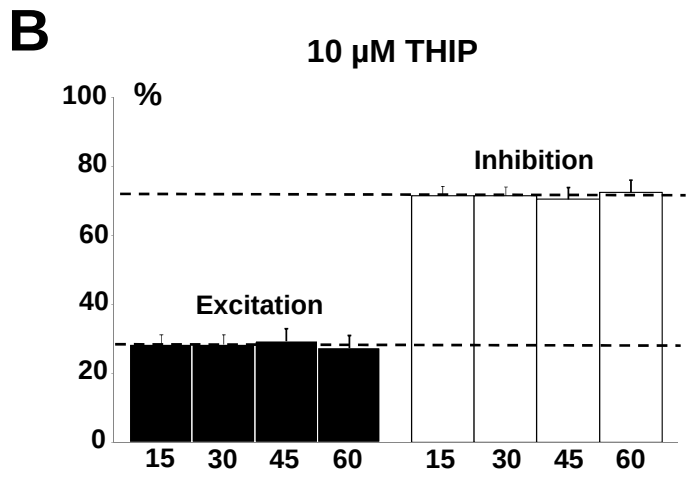
B
10 µM THIP
100
%
80
60
40
20
0
Inhibition
Excitation
15
30
45
60
15
30
45
60

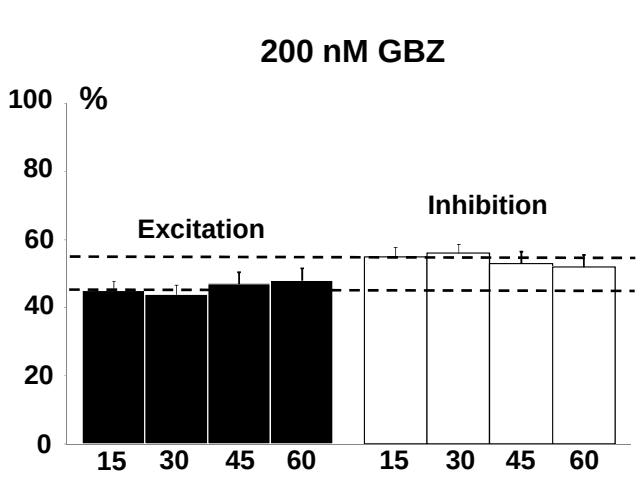
C
200 nM GBZ
100
%
80
60
40
20
0
Excitation
Inhibition
15
30
45
60
15
30
45
60

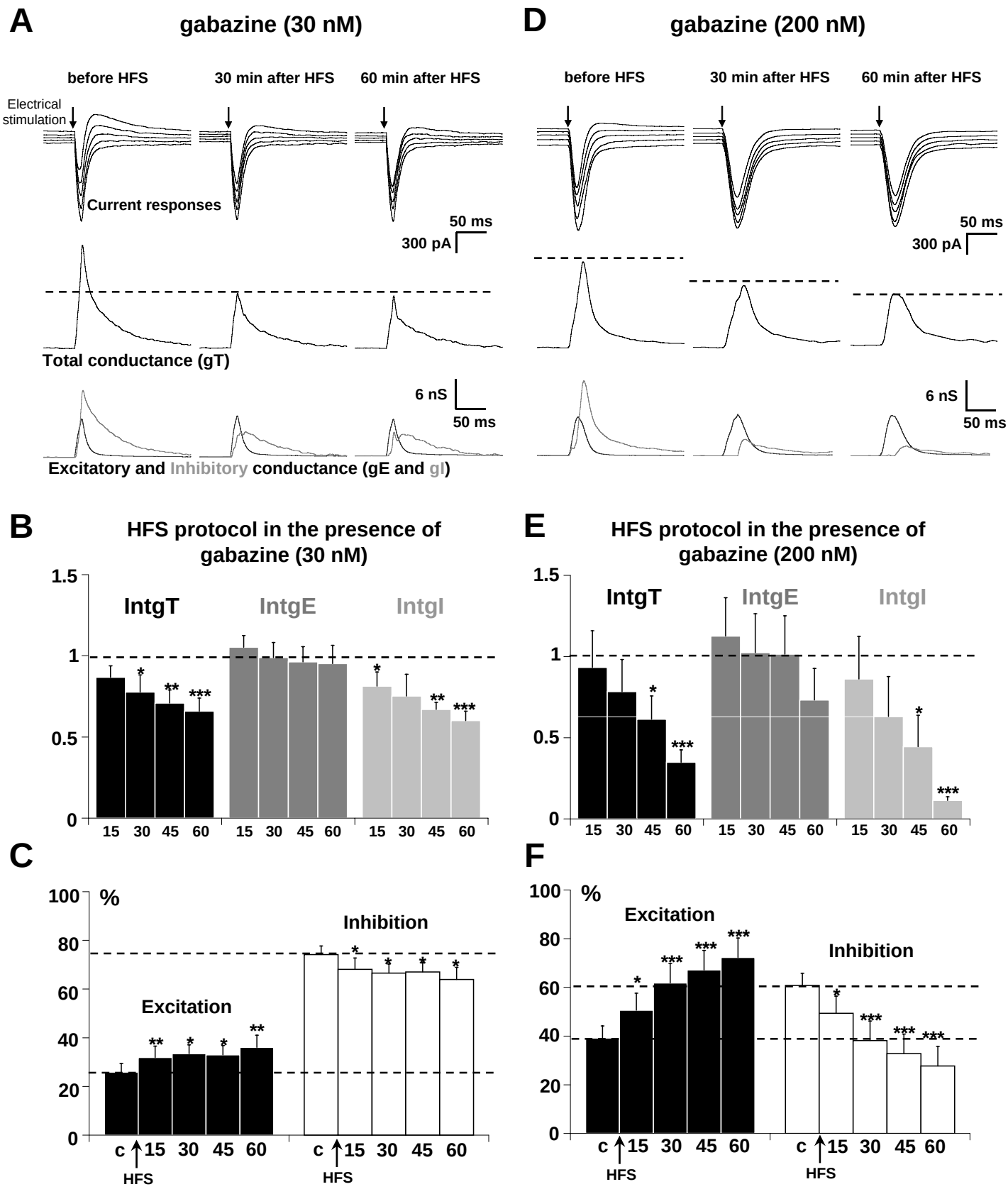
A
gabazine (30 nM)
before HFS
30 min after HFS
60 min after HFS
Electrical stimulation
Current responses
50 ms
300 pA
Total conductance (gT)
6 nS
50 ms
Excitatory and Inhibitory conductance (gE and gI)
D
gabazine (200 nM)
before HFS
30 min after HFS
60 min after HFS
50 ms
300 pA
6 nS
50 ms
B
HFS protocol in the presence of gabazine (30 nM)
IntgT
IntgE
IntgI
1.5
1
0.5
0
15 30 45 60 15 30 45 60 15 30 45 60
E
HFS protocol in the presence of gabazine (200 nM)
IntgT
IntgE
IntgI
1.5
1
0.5
0
15 30 45 60 15 30 45 60 15 30 45 60
C
100
%
80
60
40
20
0
Inhibition
Excitation
c 15 30 45 60 c 15 30 45 60
HFS
HFS
F
100
%
80
60
40
20
0
Excitation
Inhibition
c 15 30 45 60 c 15 30 45 60
HFS
HFS

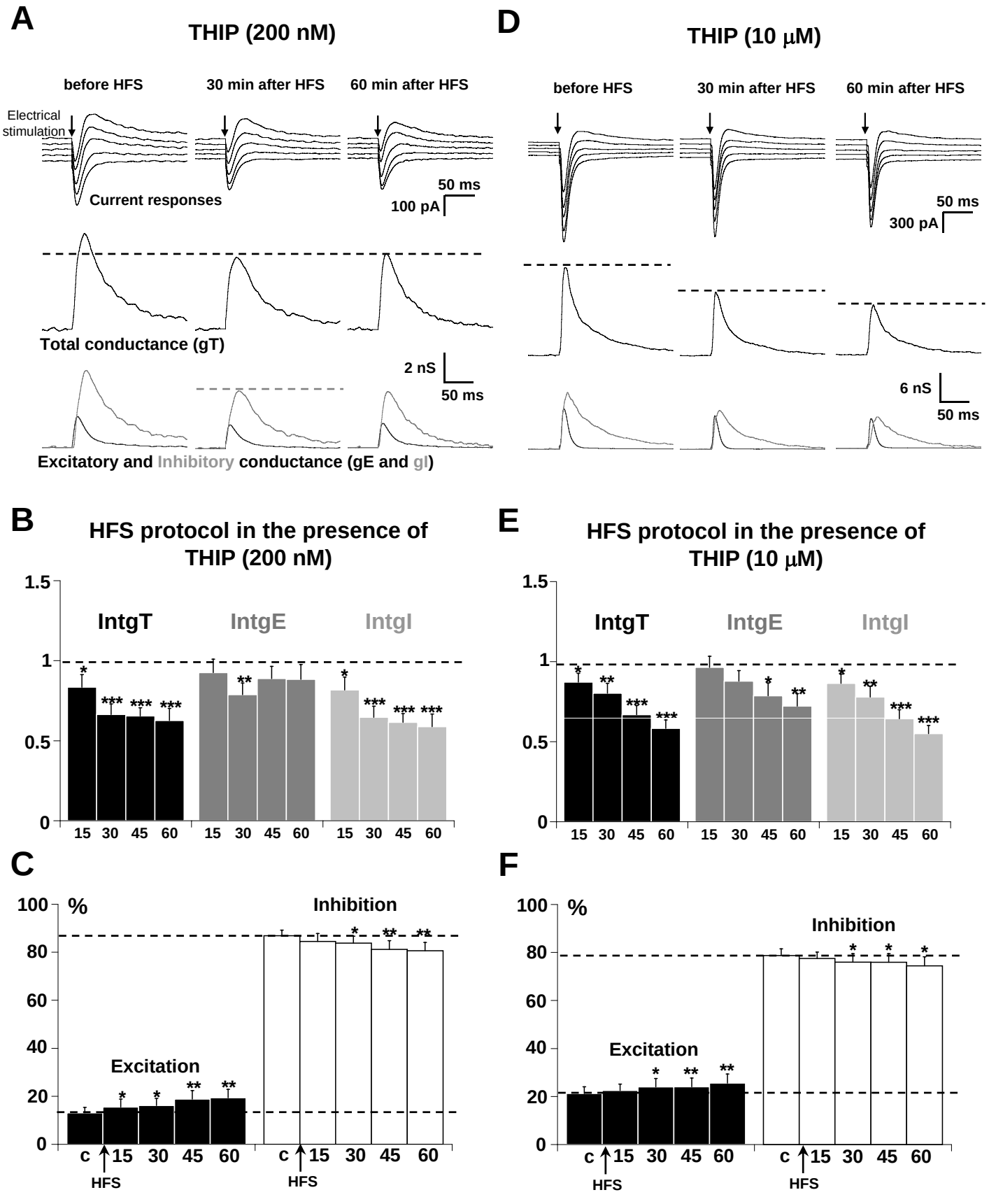
A
THIP (200 nM)
before HFS
30 min after HFS
60 min after HFS
Electrical stimulation
Current responses
50 ms
100 pA
Total conductance (gT)
2 nS
50 ms
Excitatory and Inhibitory conductance (gE and gI)
D
THIP (10 μM)
before HFS
30 min after HFS
60 min after HFS
50 ms
300 pA
6 nS
50 ms
B
HFS protocol in the presence of THIP (200 nM)
IntgT
IntgE
IntgI
1.5
1
0.5
0
15 30 45 60 15 30 45 60 15 30 45 60
E
HFS protocol in the presence of THIP (10 μM)
IntgT
IntgE
IntgI
1.5
1
0.5
0
15 30 45 60 15 30 45 60 15 30 45 60
C
100
%
Inhibition
80
60
40
20
0
Excitation
c 15 30 45 60 c 15 30 45 60
HFS
HFS
F
100
%
Inhibition
80
60
40
20
0
Excitation
c 15 30 45 60 c 15 30 45 60
HFS
HFS

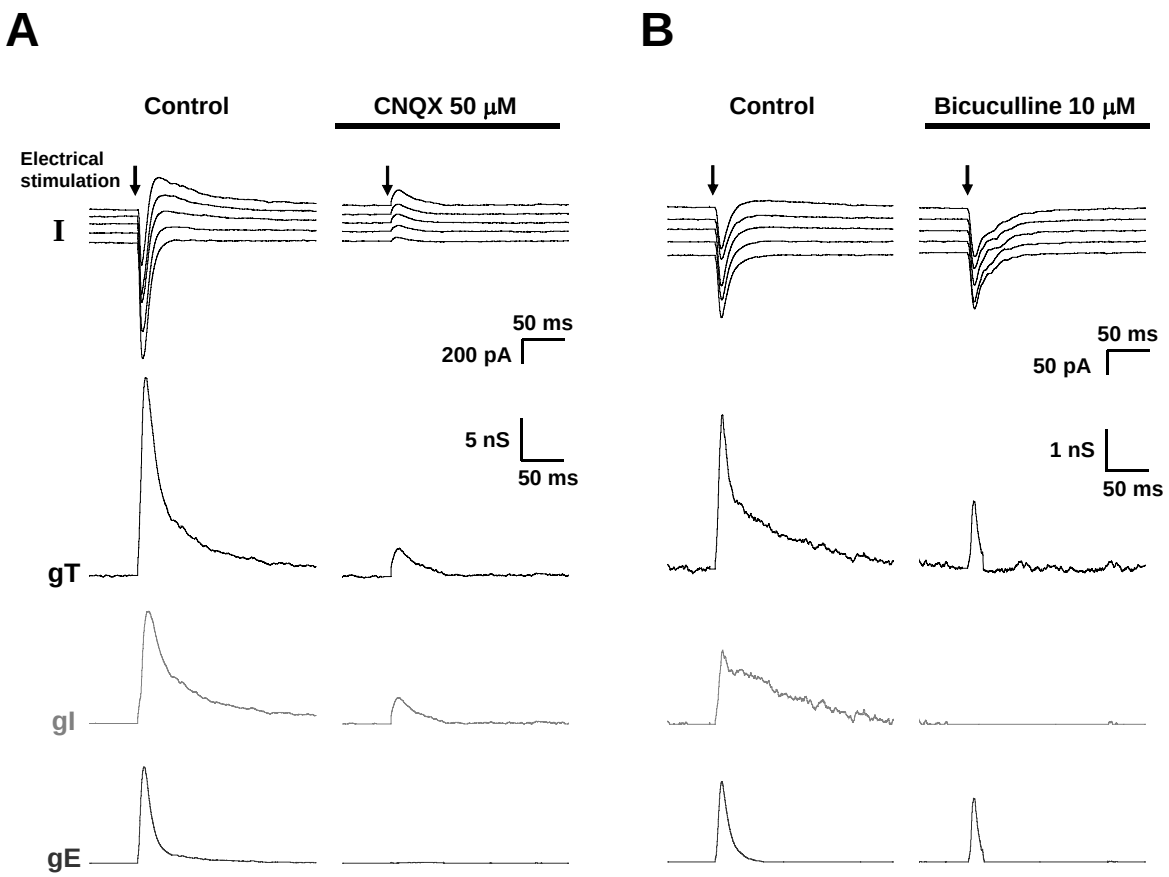
A
Control
CNQX 50 μM
Electrical stimulation
I
50 ms
200 pA
5 nS
50 ms
gT
gI
gE
B
Control
Bicuculline 10 μM
50 ms
50 pA
1 nS
50 ms